Intelligent Gamma-Ray Spectroscopy Using 3-D Position-Sensitive Detectors

Carolyn E. Lehner, *Student Member, IEEE*, Zhong He, *Senior Member, IEEE*, and Glenn F. Knoll, *Fellow, IEEE*

***Abstract*—The performance of gamma-ray spectrometers at high energies (several MeV) can be greatly improved through intelligent spectroscopic analysis if spatial information is obtained for each energy deposition. In position-sensitive detectors, the energy and three-dimensional (3-D) position of each interaction in the detector are determined. Recognizing the signatures of multiple interactions in the detector can help to reconstruct the energies of the initial gamma-rays even when the full energies are not deposited. Experimental work by our research group has demonstrated the feasibility of carrying out spatially resolved measurements of individual gamma-ray interactions throughout the volume of a CdZnTe spectrometer. We present the results of a simulation study for gamma-rays incident upon a 6-cm^3 CdZnTe detector using two reconstruction methods: high-efficiency intelligent spectroscopy (HEIS) in which the peak-to-total ratio is greatly improved relative to traditional spectroscopy while maintaining almost the same intrinsic peak efficiency; and peak-only intelligent spectroscopy (POIS) in which the peak-to-total ratio can approach 0.9, assuming realistic values for energy resolution. Although POIS reduces the intrinsic peak efficiency, it will significantly improve the signal-to-noise ratio for many measurements. The predicted performance is unprecedented for a detector of such small volume and illustrates the gains that can be expected by exploiting 3-D information.**

***Index Terms*—Gamma-ray detector, intelligent spectroscopy, position-sensitive detectors, three-Compton reconstruction.**

I. Introduction

Traditionally, the performance of a gamma-ray spectrometer has been limited by the energy resolution and sensitivity of the detector. To improve the performance, many efforts have concentrated on suppressing the Compton background, which dominates the spectrum for gamma-rays with energies above a few hundred keV in most detector materials. One common method is to implement anti-coincidence techniques, which require a second detector and reduce the detector field of view. Compton suppression in a single detector has also been performed using energy cutoff techniques [1]. However, the efficiency of such systems is always reduced.

Position-sensitive detectors in which the three-dimensional (3-D) interaction locations and deposited energies can be determined provide additional information about the gamma-ray source. With 3-D detectors it is possible to reconstruct the original gamma-ray energy using Compton scatter kinematics [2], [3]. This is a useful technique for intermediate gamma-ray energies (few hundred keV), but the algorithm does not account for the pair production processes that occur at higher energies (several MeV).

Following our preliminary work on improving detector performance using 3-D position and energy information [4], we present two algorithms for intelligent spectroscopy that use the information available from position-sensitive detectors to reconstruct incident gamma-ray energies above the pair production threshold. The first algorithm—high efficiency intelligent spectroscopy (HEIS)—is used to maximize the efficiency, which can equal or exceed that of a traditional spectroscopy system. The second algorithm—peak-only intelligent spectroscopy (POIS)—is used to improve the spectral response function. These methods are independent of detector geometry and material and can be implemented for any 3-D detector system. They can be implemented in parallel with the usual spectroscopy technique of summing energy depositions at multiple sites. Thus one can display three separate spectra that relate in different ways to the incident energy spectrum of the gamma-rays.

To demonstrate the benefits of intelligent spectroscopy the performance of these algorithms is reported for a simulated 2 cm $\times$ 2 cm $\times$ 1.5 cm CdZnTe detector and compared to traditional spectroscopy techniques. We examine the effectiveness of the algorithms for different gamma-ray energies and detector energy and position resolutions. Finally, a realistic source is modeled and analyzed. This work is motivated by our current research with 3-D position-sensitive CdZnTe detectors (see for example [5], [6]).

II. Spectroscopy Algorithms

A. Traditional Spectroscopy

In traditional spectroscopy, the only information available is the total energy deposited in the detector by an incident gamma-ray. All interaction sequences in the detector that deposit any energy, regardless of the quantity, are accepted in the energy spectrum. Thus, any sequence of interactions that does not deposit full energy results in extraneous features in the spectrum such as the Compton continuum or single and double escape peaks.

B. High Efficiency Intelligent Spectroscopy

High efficiency intelligent spectroscopy (HEIS) can be used to eliminate much of the extraneous spectrum features while maintaining an intrinsic peak efficiency near (or even larger than) that of traditional spectroscopy. Hence the information about the true gamma-ray energy is preserved while the Compton continuum and escape peaks are reduced. HEIS is performed on an event-by-event basis with no *a priori* knowledge of incident gamma-ray energy or direction. The algorithm

Manuscript received December 2, 2002; revised April 8, 2003. This research was performed under appointment to the U.S. Department of Energy Nuclear Engineering and Health Physics Fellowship Program sponsored by the U.S. Department of Energy's Office of Nuclear Energy, Science, and Technology.

The authors are with the are with the Department of Nuclear Engineering and Radiological Sciences, University of Michigan, Ann Arbor, MI 48109 USA (e-mail: clehner@umich.edu; hezhong@umich.edu; gknoll@umich.edu).

Digital Object Identifier 10.1109/TNS.2003.814583

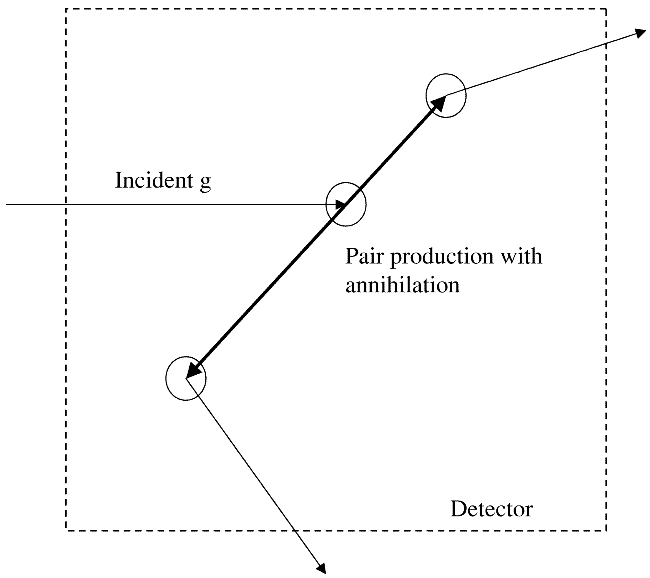

Fig. 1. The alignment of pair production sequences. The annihilation photons are emitted in nearly opposite directions, yielding a line of three interaction points. The center point is the initial pair production event.

is a series of *if-else if* statements that can be implemented in any data analysis program in list-mode or real-time operation.

There are three pieces of information available for each interaction sequence in the detector: the number of events, the energy deposited in each event, and the 3-D location of each event. The reconstruction technique differs depending on the number of interactions observed.

1) Single-event sequences: All sequences with only one interaction are discarded. Thus, the single-scatter Compton continuum and most of the double escape peak are eliminated. There will also be some efficiency loss due to photoabsorptions that are discarded, but as gamma-ray energy increases the probability of depositing full energy in one interaction sharply decreases and the effect is small.

2) Double-event sequences: First, check for either event depositing energy equivalent to the electron rest mass, m_ec^2 (511 keV). This most likely corresponds to the photoabsorption of a photon resulting from the annihilation of positrons generated in pair production interactions. If one event is observed to deposit m_ec^2, then $2m_ec^2$ is automatically added to the other energy. Thus, the gamma-ray energy can be correctly reconstructed for any two-event sequence in which a pair production occurs, followed by positron annihilation in which one of the photons is immediately absorbed. If neither event deposited m_ec^2, then the two energies are summed, as in traditional spectroscopy.

3) Triple-event sequences: Check for any of the events depositing m_ec^2. If observed, add $2m_ec^2$ to higher of the other two energies. Also check for any two events summing to m_ec^2, and add $2m_ec^2$ to the remaining energy. This corresponds to a pair production sequence in which one annihilation photon escapes while the other scatters and is then absorbed. If these are not observed, then check the alignment of events. As shown in Fig. 1, the interaction locations should lie approximately on a line if each annihilation photon is scattered once before leaving the detector. In this case, the central event corresponds to the initial pair production, and $2m_ec^2$ is added to the energy deposited there. (The effectiveness of this method is subject to the finite deceleration distance of the positron and the angular correlation of the annihilation photons.) If none of the above applies, three-Compton reconstruction is performed for the six possible sequence orders. If any of the reconstructed gamma-ray energies is equal to the sum of the energies deposited, then the energies are summed. Thus, we use three-Compton reconstruction to verify that the full energy was deposited in a sequence of Compton scatters and a photoabsorption. If none of the above applies, then the sequence is rejected. At this point, we have reconstructed the gamma-ray energy for most three-event sequences involving pair production, and we have accounted for every sequence that deposits full energy.

4) Quadruple-event sequences: We extend the three-event analysis to four events. First, check for any one, two, or three events whose energies sum to m_ec^2. If observed, add $2m_ec^2$ to the highest energy remaining. For all possible sequences, check the alignment of the first three events, and reconstruct as before if they lie on a line. For each group of three events, perform three-Compton reconstruction, and compare the reconstructed energies to the sum of all the energies. If none of the above applies, reject the sequence.

5) Sequences with more than four events: It is simple to extend the analysis for more than four events. However, the computation time may become prohibitively long and the contribution to the spectrum will be minimal for high-Z detector materials in which the number of interactions can be expected to be relatively low. Thus, for any sequence involving more than four events the energies are simply summed in the HEIS algorithm.

With this procedure we have tried to relocate to the full-energy peak the sequences that lead to single escape peaks in the traditional energy spectrum. We have also eliminated most of the double escape peaks and all of the single-scatter Compton continuum. When sequences could not be identified as having a pair production, three-Compton reconstruction is performed. Finally, energies are summed for sequences that could lead to a full energy event but do not satisfy the other criteria. There are some sequences that will reconstruct incorrectly using this method, although their probability of occurrence is small. For example, in any sequence that begins with a Compton scatter event and has an identifiable pair production event, adding $2m_ec^2$ to the energy of the appropriate event will not account for the energy deposited in the initial scatter. However, the relative probability of occurrence is small compared with that of a sequence that begins with a pair production event. Also, a sequence in which about 511 keV is deposited in a Compton scatter will be reconstructed as if a pair production occurred. Despite these incorrectly reconstructed sequences, the HEIS algorithm reduces the extraneous features in the spectrum while retaining a peak efficiency near that of traditional spectroscopy.

C. Peak-Only Intelligent Spectroscopy

POIS is useful for applications in which a near-perfect response function is desired. The Compton continuum and escape peaks usually present in the energy spectrum are nearly eliminated because the accepted sequences are those in which the full gamma-ray energy can be reconstructed. As in HEIS, there is no *a priori* knowledge of gamma-ray energy or source direction.

The POIS and HEIS methods are identical with one exception. For sequences in which the HEIS algorithm sums the energies deposited if no other criterion is satisfied, in POIS these sequences are rejected. As in HEIS, the POIS algorithm could be extended beyond four interactions. However, the contribution to the spectrum will be minimal for high-Z materials. Thus, all sequences with more than four events are discarded in order to

TABLE I
SUMMARY OF HEIS AND POIS METHODS

No. Events	HEIS	POIS
1	Reject all.	Reject all.
2	If $E=m_ec^2$, add $2m_ec^2$ to other energy. Else, sum energies.	If $E=m_ec^2$, add $2m_ec^2$ to other energy. Else, reject.
3	If $E=m_ec^2$,add $2m_ec^2$ to higher remaining energy. Else if $\Sigma E=m_ec^2$, add $2m_ec^2$ to remaining energy. Else if 3 events are aligned, add $2m_ec^2$ to middle energy. If ΣE=Triple Compton energy, sum energies. Else, reject.	If $E=m_ec^2$,add $2m_ec^2$ to higher remaining energy. Else if $\Sigma E=m_ec^2$, add $2m_ec^2$ to remaining energy. Else if 3 events are aligned, add $2m_ec^2$ to middle energy. If ΣE=Triple Compton energy, sum energies. Else, reject.
4	If $E=m_ec^2$, add $2m_ec^2$ to highest remaining energy. Else if $\Sigma E=m_ec^2$, add $2m_ec^2$ to remaining energy. Else if 3 events are aligned, add $2m_ec^2$ to middle energy. Else if ΣE=Triple Compton energy, sum energies. Else, reject.	If $E=m_ec^2$, add $2m_ec^2$ to highest remaining energy. Else if $\Sigma E=m_ec^2$, add $2m_ec^2$ to remaining energy. Else if 3 events are aligned, add $2m_ec^2$ to middle energy. Else if ΣE=Triple Compton energy, sum energies. Else, reject.
4+	Sum energies.	Reject all.

TABLE II
MOST LIKELY SEQUENCE PROBABILITIES AND HEIS RECONSTRUCTION PROCESSES FOR 2.5 MEV GAMMA RAYS

No. Events	Event Sequence	Per incident gamma ray	Per detected gamma ray	Accept?[a]	Process
1	Compton	0.1800	0.6334	R	Reject singles
	Pair	0.0202	0.0710	R	Reject singles
	Photo	0.0049	0.0173	R	Reject singles
	Accepted single-site events	0.0000	0.0000		
2	Compton-Compton	0.0297	0.1046	A	Sum energies
	Compton-Photo	0.0135	0.0474	$\underline{A}$	Sum energies
	Pair-Escape-Compton	0.0060	0.0212	A	Sum energies
	Pair-Escape-Photo	0.0024	0.0083	$\underline{A}$	Detect 511
	Accepted double-site events	0.0520	0.1831		
3	Compton-Compton-Photo	0.0096	0.0337	$\underline{A}$	Three-Compton
	Compton-Compton-Compton	0.0048	0.0168	R	Reject
	Pair-Escape-Compton-Photo	0.0025	0.0089	$\underline{A}$	Detect 511 sum
	Pair-Escape-Compton-Compton	0.0011	0.0038	R	Reject
	Accepted triple-site events	0.0138	0.0487		
4	Compton-Compton-Compton-Photo	0.0042	0.0147	$\underline{A}$	Three-Compton
	Pair-(Compton-Compton)-Compton	0.0012	0.0041	$\underline{A}$	Alignment
	Compton-Compton-Compton-Compton	0.0007	0.0025	R	Reject
	Pair-Escape-Compton-Compton-Photo	0.0005	0.0019	$\underline{A}$	Detect 511 sum
	Accepted quadruple-site events	0.0063	0.0223		
	Total accepted events	0.0722	0.2541		

Probabilities are given for a 2 cm x 2 cm x 1.5 cm CdZnTe detector.
[a] A and R indicate accepted and rejected sequences, respectively, for the HEIS method. $\underline{A}$ indicates an accepted sequence that contributes to the full-energy peak.

maintain the best possible spectral response while minimizing execution time.

The POIS and HEIS methods are summarized in Table I.

III. IDEAL ALGORITHM PERFORMANCE

To test the ideal performance of the intelligent spectroscopy methods, we simulated a CdZnTe detector using the Geant4 simulation package [7]. A flood source of monoenergetic 2.5 MeV gamma-rays was incident on the square face of a 2 cm $\times$ 2 cm $\times$ 1.5 cm block of $Cd_{0.9}Zn_{0.1}Te$. Detector housing and electronics were neglected in the geometry. Coherent and incoherent scatter, photoelectric absorption, and pair production were all modeled in the simulation. The effects of finite electron momentum were not modeled, although they could be estimated by introducing an additional uncertainty in the measured energies according to the physics of Doppler broadening. (For 511 keV, the maximum Doppler contribution is nearly 6 keV full width at half maximum (FWHM) or roughly 1%, and the percent contribution decreases with increasing energy). Coincidences involving multiple incident gamma-rays were neglected. Charge transport and collection effects were ignored. The electron cloud size can be incorporated into the position resolution, and is expected to be one the order of 1 mm for 2 MeV pho-

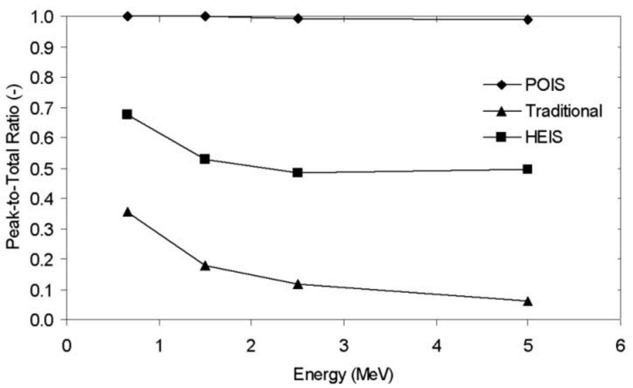

Fig. 2. Peak-to-total ratios calculated for ideal spectroscopy performance on a $2 \times 2 \times 1.5\ \mathrm{cm}^3$ CdZnTe detector assuming perfect energy and position resolution and flawless execution of the algorithm.

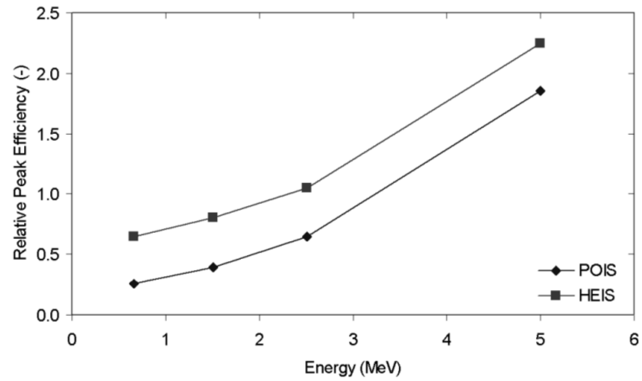

Fig. 3. Relative peak efficiency compared to traditional spectroscopy calculated for ideal spectroscopy case. The HEIS method shows better efficiency performance at and above 2.5 MeV than traditional spectroscopy.

tons. In the ideal case, perfect position and energy information were assumed, thereby neglecting both Doppler broadening and electron cloud size effects. Thus, the ideal case tests the intelligent spectroscopy methods without the influence of imperfect application of the algorithms or of finite position and energy resolutions. (These influences are discussed in Sections IV and V.)

The ideal performance was determined as follows. The probabilities were calculated for each possible gamma-ray sequence up to four events. Any sequence that should reconstruct correctly (for example, a sequence involving first a pair production followed by a single escape and absorption of the other annihilation photon) was assumed to contribute to the photopeak. A sequence in which two Compton scatters occur, followed by a Rayleigh scatter and photoabsorption would not reconstruct correctly for POIS. In this latter case, the three-Compton technique would fail due to the direction change associated with the Rayleigh scatter. In both algorithms, this sequence would be rejected.

Table II lists the most likely sequences for up to four events. The probability of each sequence occurring in the CdZnTe detector (without the interference of coherent scatter) is given per incident and per detected 2.5 MeV gamma-ray. Each sequence is designated as accepted or rejected by the HEIS algorithm and those sequences leading to reconstruction of the full gamma-ray energy are underlined. In addition, the total fraction of events accepted by the algorithm is given. The POIS algorithm yields similar results except that the first three two-event sequences would be rejected. The sequence probabilities indicate that the efficiency loss from rejecting single photoelectric events is compensated by detecting annihilation photons and relocating to the full-energy peak those sequences that would otherwise have been in the single- escape peak. Also note that single Compton scatter contributes over 60% of the traditional energy spectrum while providing no information about the gamma-ray energy; these events are rejected in both HEIS and POIS methods.

For spectra from monoenergetic sources, two quantities are reported to demonstrate the effectiveness of the methods: peak-to-total ratio and relative peak efficiency compared to traditional spectroscopy. The first quantity measures the improvement in the spectral response function, and the second measures the change in detection efficiency. The peak-to-total ratios are shown in Fig. 2 for selected energies from 662 keV to 5 MeV. Fig. 3 shows the relative peak efficiency compared to traditional spectroscopy.

In the ideal case, HEIS and POIS easily outperformed traditional spectroscopy for high gamma-ray energies. At 2.5 MeV, the POIS method yielded nearly two-thirds the efficiency of traditional spectroscopy. The peak-to-total ratio was almost perfect because only those events that are known to contribute to the photopeak are accepted. The only sequences incorrectly reconstructed with POIS in the ideal case are those that begin with a Compton scatter, followed by an identifiable pair production, as previously discussed. Above 2.5 MeV HEIS yielded an efficiency above that of traditional spectroscopy, while increasing the peak-to-total ratio by at least a factor of 4. Note that the gain in performance increased with incident gamma-ray energy.

There was some loss in efficiency for gamma-ray energies near or below the pair production threshold. These algorithms are designed for high-energy spectroscopy, so this is no surprise. However, there was still significant improvement at 662 keV in the peak-to-total ratio for both HEIS and POIS algorithms. For applications in which a variety of gamma-ray energies are present, the reduction in Compton background may outweigh the efficiency loss at low energies.

IV. Influence of Finite Energy Resolution

The performance of the intelligent spectroscopy algorithms discussed here depends on the ability to detect, among other things, a photon with energy $m_e c^2$. The energies deposited in each interaction must be compared to some window of acceptable energies centered around 511 keV. Thus, there will be a finite number of photons that deposit energy within the acceptable window that are not the result of positron annihilation. The size of the window, and thus the number of incorrectly reconstructed gamma-ray energies, is determined by the energy resolution of the system. We expect the performance to be worse than predicted in the ideal case and to degrade as energy resolution gets worse.

To model these effects simulations were performed as before except a Gaussian spread was introduced in the energies by assuming the resolution to be a constant fraction of the energy deposited. This assumption is conservative in that for most detector systems the energy resolution expressed as a percentage decreases with increasing energy. Doppler broadening was not explicitly considered, although it can be estimated by noting the

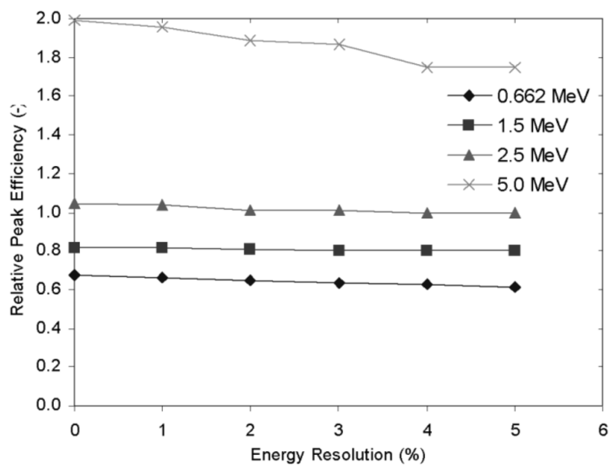

Fig. 4. The relative peak efficiencies calculated for HEIS method as a function of energy resolution For 2.5 and 5.0 MeV, HEIS nearly always yielded a higher efficiency than traditional spectroscopy.

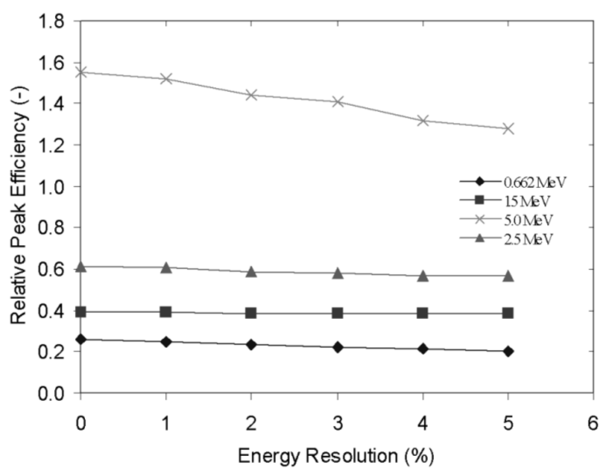

Fig. 5. The relative peak efficiencies calculated for POIS method as a function of energy resolution. At 5 MeV POIS yielded a higher efficiency than traditional spectroscopy.

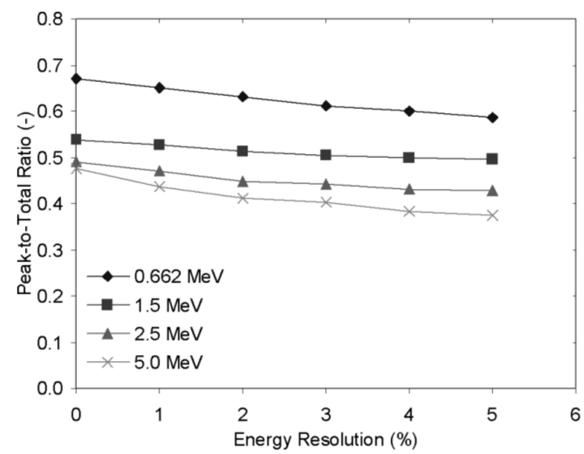

Fig. 6. Peak-to-total ratios calculated for HEIS method as a function of energy resolution. The algorithm shows better peak-to-total ratios for low energies than for high energies.

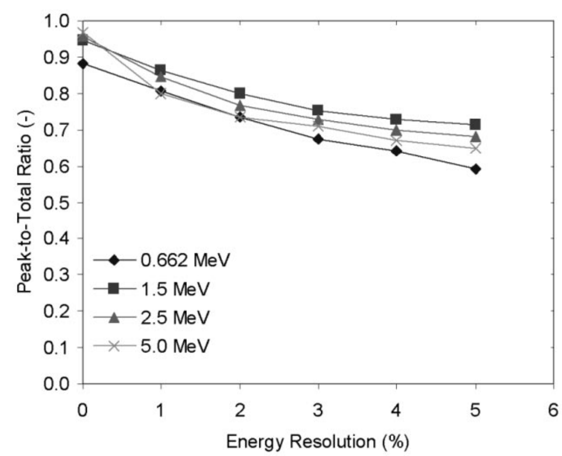

Fig. 7. The peak-to-total ratios calculated for POIS method as a function of energy resolution at selected gamma-ray energies. The peak-to-total ratio decreased with energy resolution and differed minimally when the incident gamma energy increased.

maximum contribution for 511 keV gamma-rays is nearly 6 keV FWHM. At 1 MeV, the maximum uncertainty due to Doppler is about 9 keV FWHM. The relative peak efficiencies obtained with HEIS and POIS algorithms are shown in Figs. 4 and 5, respectively. As observed in the ideal case, the efficiency of the HEIS method met or exceeded that of traditional spectroscopy above 2.5 MeV. As resolution degraded to 5%, the efficiency for HEIS remained above 88% of the value obtained with perfect energy resolution for all energies. In POIS, the efficiency degradation was more severe with values dropping to about 78% in the same comparison. Both methods use three-Compton reconstruction, which has an effectiveness that is severely dependent on energy resolution. For all energies, the efficiency is decreased as energy resolution increases due to the size of the acceptance windows used in the algorithm. It is necessary to compromise between obtaining high efficiency and good spectral response in selecting these windows. Larger acceptance windows will increase efficiency, but also allow more incorrectly reconstructed sequences, thus decreasing the peak-to-total ratio. These window parameters will have to be optimized for a given detector and application.

The peak-to-total ratios for HEIS and POIS are shown in Figs. 6 and 7, respectively. The largest effect observed in HEIS was for 5.0 MeV, where the peak-to-total decreased from 0.48 to 0.38. HEIS performed reasonably well for any energy resolution tested. In POIS the peak-to-total ratio dropped from 0.88 to 0.59 for 662 keV gamma-rays as resolution worsened. At 5 MeV it decreased from 0.97 to 0.65. For comparison the peak-to-total for traditional spectroscopy is only 0.07 for 5 MeV gamma-rays. Thus, both HEIS and POIS algorithms show greatly improved performance compared with traditional spectroscopy.

V. Influence of Finite Position Resolution

Position resolution will also have some effect on the performance of intelligent spectroscopy especially at high energies. Both the pair production alignment and three-Compton reconstruction routines require a calculation of angles based on the interaction positions. The accuracy of the calculations depends on the position resolution of the system.

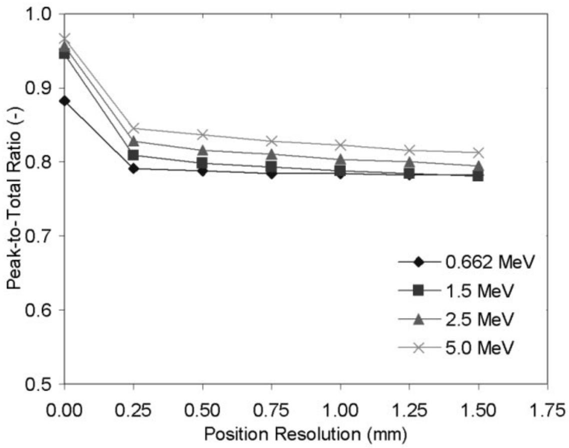

Fig. 8. Peak-to-total ratios calculated for POIS method as a function of position resolution.

We performed simulations assuming perfect energy resolution in which the position of interactions was spread using a constant-width Gaussian distribution. As with energy resolution, position resolution is measured in terms of the FWHM. In practice, the use of pixellated detectors leads to discrete positions, rather than Gaussian distributions. This may lead to some reconstruction artifacts not observed here. However, we seek to demonstrate the principles of intelligent spectroscopy without limiting the analysis to pixellated devices.

Position resolution has a pronounced effect on both the alignment of pair production events and the three-Compton reconstruction. In the latter, it is necessary to calculate the scattering angle of the second interaction. The accuracy of this angle calculation is limited by the position resolution. Three-Compton reconstruction is a significant factor in the POIS algorithm because it can provide for up to 10% of the total peak efficiency at 5 MeV. In HEIS, three-Compton reconstruction contributes a smaller percentage of the total peak efficiency and, thus, the behavior of the algorithm is much less dependent on position resolution than in the POIS method. The HEIS and POIS methods showed almost no change in efficiency as position resolution worsens because the acceptance windows have been chosen to maintain efficiency for all position resolutions considered. Thus, the relative efficiencies were equivalent to those calculated in the perfect energy resolution case above. The peak-to-total ratios in HEIS minimally decreased as position resolution worsens. In POIS, the effect was more dramatic. The POIS peak-to-total ratios are shown in Fig. 8. POIS showed a reduction of 11%–17% in the peak-to-total ratio for all energies as position resolution degraded from 0.0 to 1.5 mm. In the worst case at 662 keV, the peak-to-total ratio was still near 0.80, indicating an excellent spectral response function.

To visually demonstrate the improvement in spectral response, the calculated energy spectra for 2.5 MeV gamma-rays are shown in Fig. 9. A 2% energy resolution and 1-mm position resolution were assumed. The POIS method yielded almost no continuum compared with traditional spectroscopy, although the intrinsic peak efficiency is reduced by one-half. As expected, HEIS is indistinguishable from the traditional spectrum in the peak region, and the Compton continuum was significantly reduced.

There is one added feature when using these intelligent spectroscopy methods: inverse escape peaks. These peaks occur 511 keV above the full-energy peak and are due to incorrectly registering a Compton event with deposited energy near $m_e c^2$ as a pair production event. Like escape peaks normally found in energy spectra, these inverse escape peaks are easily identifiable by their location. The intensity of the inverse peaks is much smaller than conventional escape peaks and it decreases as gamma-ray energies increase. Thus, the interference with other gamma-ray lines is minimal for high energies. For 2.5 MeV gamma-rays, the inverse escape peak is located at 3.011 MeV, which was observed in the spectra for HEIS and POIS in Fig. 9. The intensity of the inverse escape peak was similar for each intelligent spectroscopy method.

VI. Realistic Source and Conditions

The above analysis assumed monoenergetic gamma-ray sources. To test the performance of the algorithms for a realistic case, we modeled a parallel beam of gamma-rays from a ^{56}Co source incident on the square face of the detector. A 2% energy resolution and 1.0 mm FWHM position resolution were introduced into the data. Both HEIS and POIS methods were applied to the data, and the spectra are shown together with the spectrum generated with traditional spectroscopy in Fig. 10. Any unlabeled peaks in the traditional spectrum are single or double escape peaks.

The improvement in the spectrum is obvious. When intelligent spectroscopy techniques are used, the escape peaks disappear. In addition, the magnitude of the Compton continuum is greatly reduced. The gamma-ray peak at 977 keV is barely visible in the traditional spectroscopy spectrum, whereas it is clearly distinguished in the POIS spectrum due to the reduced continuum. Thus, intelligent spectroscopy can provide more information about weak gamma-ray lines than would normally be available.

The extra peak observed at 1548 keV is the inverse escape peak from the 1037 keV gamma-ray. The other inverse escape peaks are either too small to identify or coincide with other gamma-ray peaks.

To quantify the improvement in the spectrum two parameters are reported. As before, we discuss the relative peak efficiency for the major gamma-ray peaks. In addition, the peak-to-background ratio is measured. This is the number of counts in the peak divided by the number of counts below it. It is standard to assume the background is a linear function from one side of the peak to the other. All counts below that line are considered background; those above it are considered part of the peak. The Maestro MCA program was used to determine peak and background areas. There are eleven prominent peaks observed in the spectra, but these values are reported only for the four "clean" gamma-ray lines. Two full-energy peaks coincide with escape peaks in the traditional case, two more coincide with the inverse escape peaks generated with intelligent spectroscopy and some peaks are the sum of several gamma-ray energies. These peak areas are therefore overestimated. The four energies of interest are 977, 1037, 2034 (together with 2015), and 2598 keV. The peak-to-background ratios and relative peak efficiencies for these gamma-rays are given, respectively, in Tables III and IV.

As expected, the POIS method outperformed HEIS and traditional spectroscopy in terms of peak-to-background. At 977 keV, where traditional spectroscopy yielded a 0.08 peak-to-background ratio, POIS achieved 0.44. A factor of 5.5

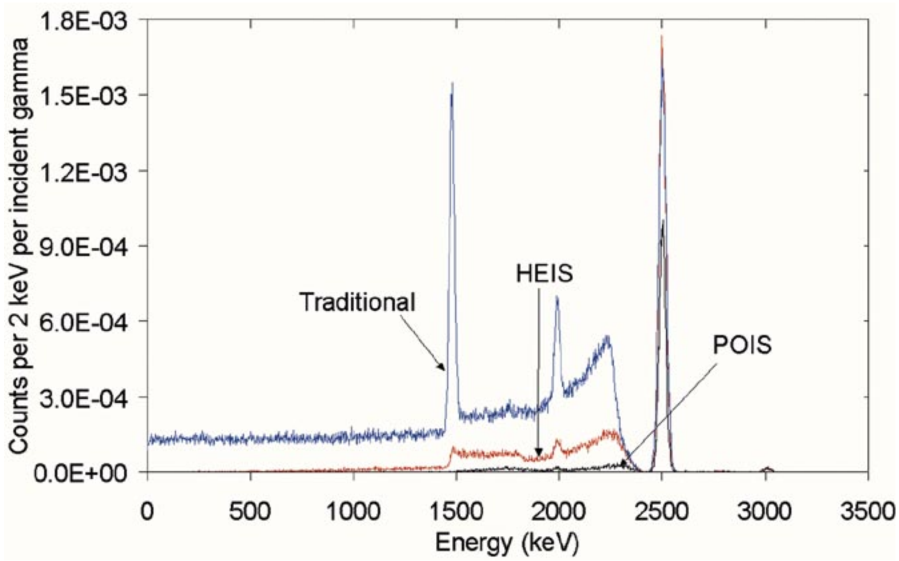

Fig. 9. Comparison of calculated spectra for 2.5 MeV gamma-rays assuming 2% energy resolution and 1-mm position resolution in a 6-cm^3 CdZnTe detector.

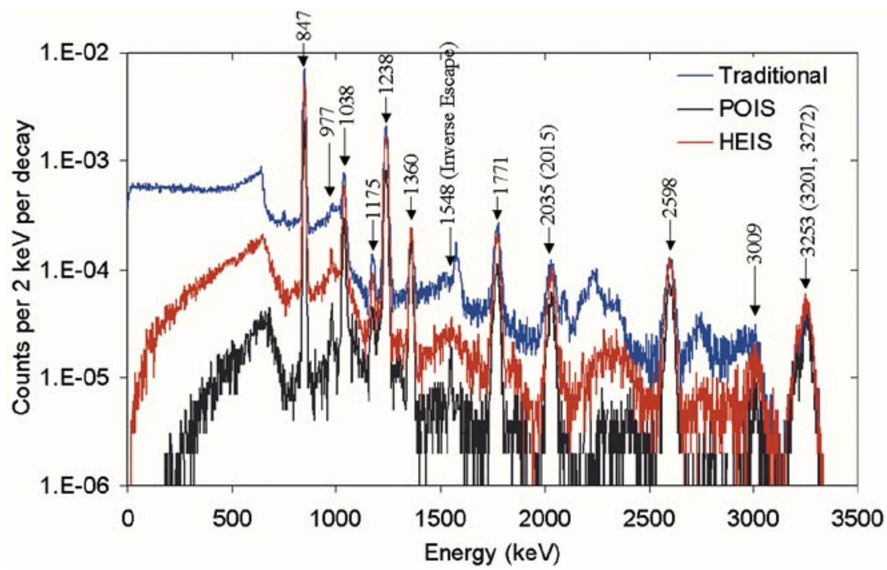

Fig. 10. Comparison of $^{56}\mathrm{Co}$ spectra generated with traditional spectroscopy, HEIS, and POIS assuming 2% energy resolution and 1-mm position resolution. The peak areas in the HEIS spectrum are nearly equal to those of the traditional spectrum, and the Compton continuum is reduced by one to two orders of magnitude in POIS compared with traditional spectroscopy.

TABLE III
PEAK-TO-BACKGROUND RATIOS CALCULATED FOR $^{56}\mathrm{Co}$

Energy (keV)	Traditional	HEIS	POIS
977	0.08	0.20	0.44
1037	0.56	1.75	3.26
2034	0.76	3.03	9.91
2598	2.58	5.62	15.23

TABLE IV
RELATIVE EFFICIENCIES CALCULATED FOR $^{56}\mathrm{Co}$

Energy (keV)	HEIS	POIS
977	0.67	0.28
1037	1.04	0.49
2034	1.10	0.66
2598	1.02	0.64

improvement in that quantity outweighed the 70% reduction in efficiency, and thus the peak was more visible in the POIS spectrum. At 2598 keV, POIS showed over five times the peak-to-background and only a 36% reduction in efficiency. For all energies above the pair production threshold HEIS resulted in nearly the same efficiency as traditional spectroscopy while increasing the peak-to-background.

The energy resolution of a photopeak obtained using intelligent spectroscopy may differ from that observed using traditional spectroscopy. Initial gamma-ray energy will have the largest role in determining the difference in energy resolution performance. For the 2.6-MeV gamma-rays from $^{56}\mathrm{Co}$ modeled above, the majority of the reconstructed events are pair production events. In these cases, the energy resolution may be improved by adding a constant $2m_ec^2$ to the measured 1.576-MeV interaction. For these events, the uncertainty (in energy units) in the full energy is then equal to the uncertainty in the measured lower energy. The resolution improves.

At the other extreme, in the spectrum for the 977-keV gamma-ray all the reconstructed events are three-Compton events because pair production does not occur. In this case, the size of the acceptance window on three-Compton events may have an adverse affect on the energy resolution observed in the spectrum. When any of the reconstructed energies is similar to the total energy deposited, it is the sum of energies that is used in the energy spectrum. We do not include any processes to determine which sequence is correct, nor do we use the reconstructed energy in the spectrum. Thus, any degradation in resolution must result from accepting sequences, by choosing a large acceptance window, which do not deposit full energy in the detector. The acceptance windows should be optimized for a given detector.

We have modeled a polychromatic source under realistic conditions and demonstrated the benefits of performing intelligent spectroscopy. It is important to note that it is not necessary to predetermine the analysis method appropriate for a specific application; these methods can be performed in parallel. For example, POIS may help identify low-energy gamma-rays in a mixed field, while traditional spectroscopy may be used to determine absolute peak efficiencies. Furthermore, the appearance or absence of various features comparing one spectrum with the others helps identify their true origin. Since these methods can be performed in real-time, the end user can use all three spectroscopy algorithms to achieve the best results for a specific application.

VII. Conclusion

We have demonstrated that improvements in spectral performance can be achieved using intelligent spectroscopy. These methods are independent of detector material and can be applied to any 3-D position-sensitive detector. The peak-to-total ratio using HEIS can be several times that of traditional spectroscopy without any significant loss in efficiency. For higher energies, the efficiency increases. We have demonstrated that POIS reduces the Compton background by one to two orders of magnitude using a realistic source, and the peak-to-background ratio is consistently higher than in traditional spectroscopy, despite the loss in overall efficiency. The specific methods we have presented work well with CdZnTe detectors for high gamma-ray energies, although it is possible that a different algorithm would perform better for other detector materials or applications.

Results obtained from a real detector will differ from those presented here for a few reasons. First, the percent energy resolution of the measurements was assumed to be constant with energy. For low energies (less than 500 keV), the uncertainty is greater than estimated here, while at high energies, the uncertainty is less. Also, Doppler broadening will change the energy uncertainty as a function of scatter angle. In pixellated detectors, charge sharing may become a problem for large energy depositions over small pixel areas. Also, the ability to precisely determine interaction energy and position degrades as the number of interactions in the 3-D CdZnTe detector increases. However, even under the worst conditions of high energy and position resolutions studies in this work, the algorithms consistently performed better than traditional spectroscopy for gamma-ray energies above the pair production threshold. The results demonstrate the gains that can be achieved by exploiting 3-D information.

References

[1] G. J. Schmid, D. Beckedahl, J. J. Blair, A. Friensehner, and J. E. Kammeraad, "HPGe compton suppression using pulse shape analysis," *Nucl. Instrum. Methods*, vol. 422A, pp. 368–372, 1999.

[2] R. A. Kroeger, W. N. Johnson, J. D. Kurfess, B. F. Phlips, and E. A. Wulf, "Three-compton telescope: Theory, simulations and performance," *IEEE Trans. Nucl. Sci.*, vol. 49, pp. 188–1892, Aug. 2002.

[3] M. W. Rawool-Sullivan, J. P. Sullivan, J. E. Koster, and B. D. Rooney, "Validity and limitations of the three-plane compton imaging technique via simulations," *IEEE Trans. Nucl. Sci.*, vol. 49, pp. 3290–3294, Dec. 2002.

[4] Z. He, C. Lehner, F. Zhang, D. K. Wehe, G. F. Knoll, J. Berry, and Y. Du, "Three-dimensional position-sensitive semiconductor spectrometers," in *Unattended Radiation Sensor Systems for Remote Applications*. Melville, NY: American Institute of Physics, 2002, vol. 632, AIP Proc., pp. 209–215.

[5] Y. F. Du, Z. He, G. F. Knoll, D. K. Wehe, and W. Li, "Evaluation of a Compton scattering camera using 3-D position sensitive CdZnTe detectors," *Nucl. Instrum. Methods*, vol. 457A, no. 1–2, pp. 203–211, 2001.

[6] Z. He, W. Li, G. F. Knoll, D. K. Wehe, J. Berry, and C. M. Stahle, "3-D position sensitive CdZnTe gamma-ray spectrometers," *Nucl. Instrum. Methods*, vol. 422A, no. 1–3, pp. 173–178, 1999.

[7] (2002) Geant4 Home Page Ver. 4.4.0. CERN Geneva, Switzerland. [Online]. Available: http://wwwinfo.cern.ch/asd/geant4/geant4.html,